Supplementary Information for

Upcycling waste commodity polymers into high-performance polyarylate materials with direct utilization of capping agent impurities

Cheng Li[1,4], Guangming Yan[2,4], ZhongwenDong[1], Gang Zhang[2,3*], and Fan Zhang[1,*]

Affiliations:

[1] National Engineering Laboratory of EcoFriendly Polymeric Materials (Sichuan), College of Chemistry, Sichuan University, Chengdu, 610064 Sichuan, PR China

[2] Institute of Materials Science and Technology, Analysis and Testing Center, Sichuan University, Chengdu, 610064 Sichuan, PR China

[3] State Key Laboratory of Polymer Materials Engineering, Sichuan University, Chengdu, 610065, China

[4] These authors contributed equally: Cheng Li, Guangming Yan.

[*] Corresponding authors. e-mail: fanzhang@scu.edu.cn; gangzhang@scu.edu.cn

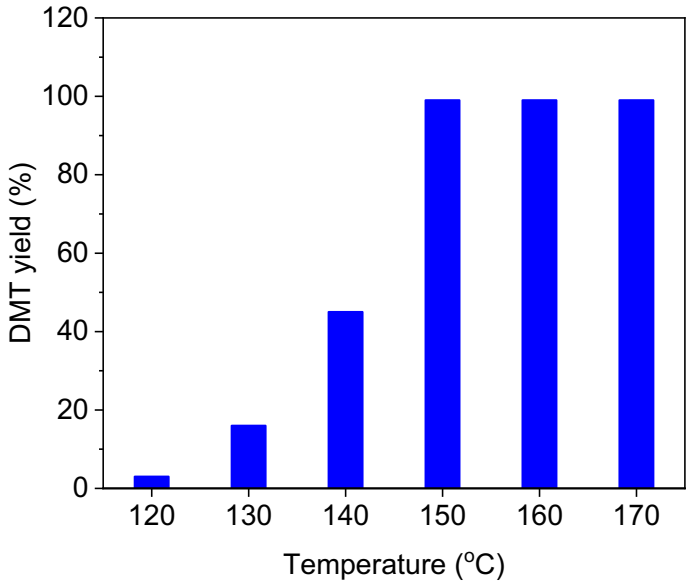

Supplementary Fig. 1 The effect of temperature on PET methanolysis. Condition: [TBDH]Ac (0.25 mmol), PET (0.5 g), MeOH (2 mL), 4 h.

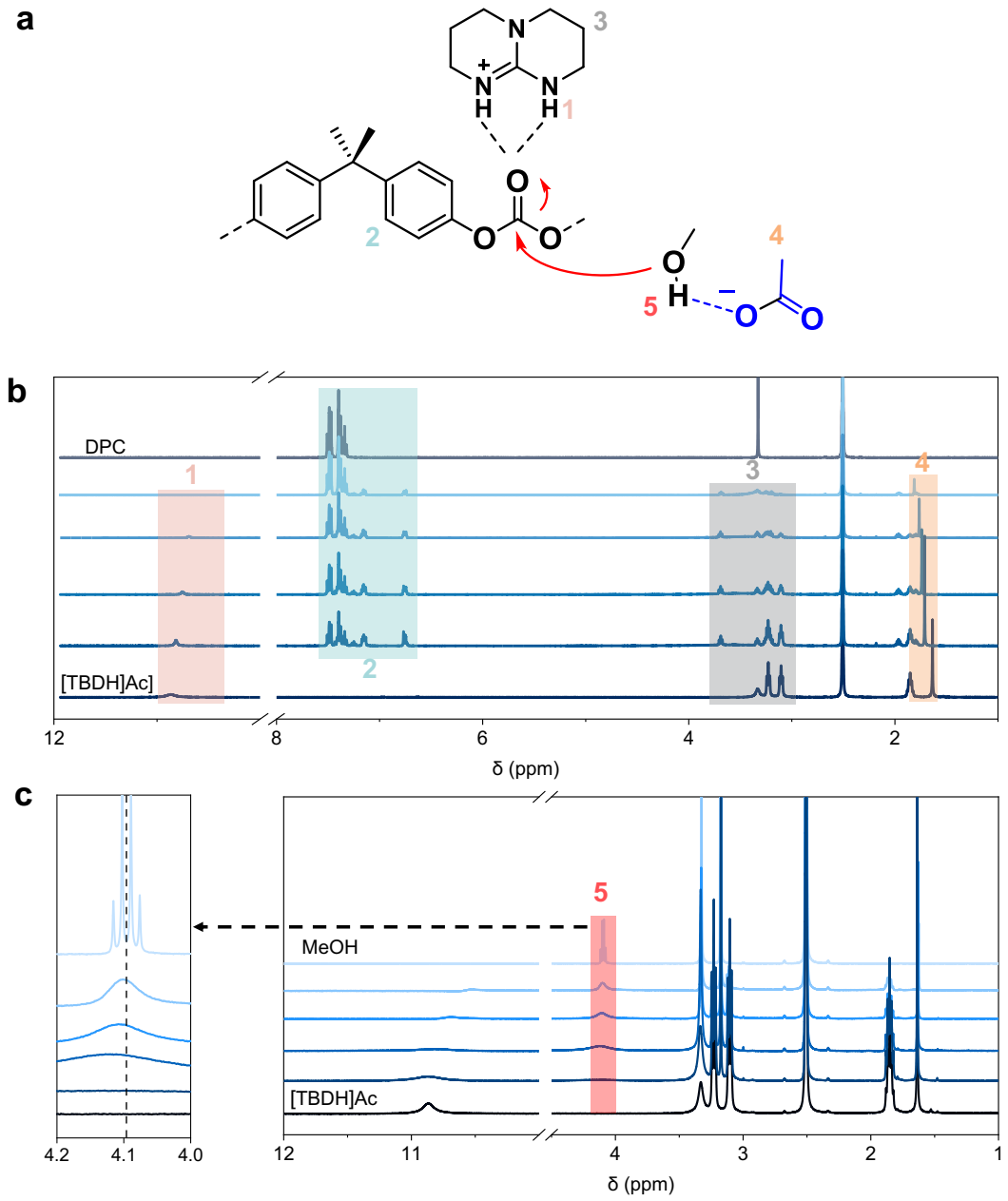

Supplementary Fig. 2 ^{1}H NMR characterization of possible hydrogen bonds. (a) Modelled dual activation mechanism for PC and methanol by [TBDH]Ac. (b) ^{1}H NMR spectra of the interaction between [TBDH]Ac and MeOH, according to the order of spectrum from top to bottom, mole ratio of [TBDH]Ac/MeOH was 0/1, 1/20, 1/10, 1/5, 1/3.33, and 1/0 in DMSO-d_6. (c) ^{1}H NMR spectra of the interaction between [TBDH]Ac and DPC, the mole ratio of [TBDH]Ac/DPC was 0/1, 1/5.6, 1/2.8, 1/1.4, 1/0, and 1/0 in DMSO-d_6.

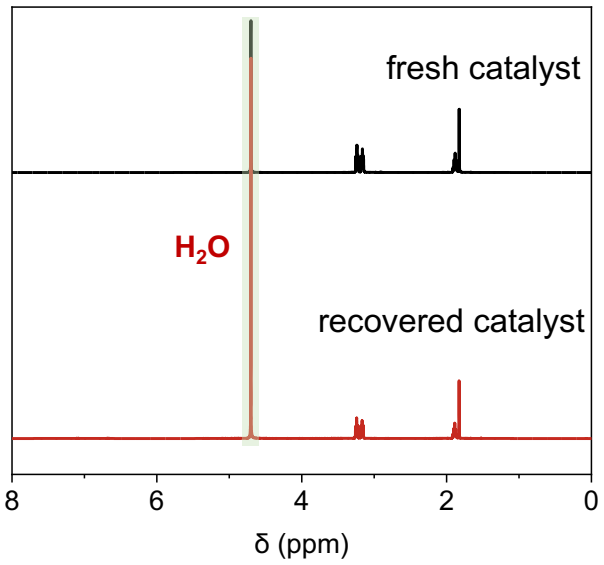

Supplementary Fig. 3 ^{1}H NMR spectra of [TBDH]Ac before and after five reaction runs in D_2O.

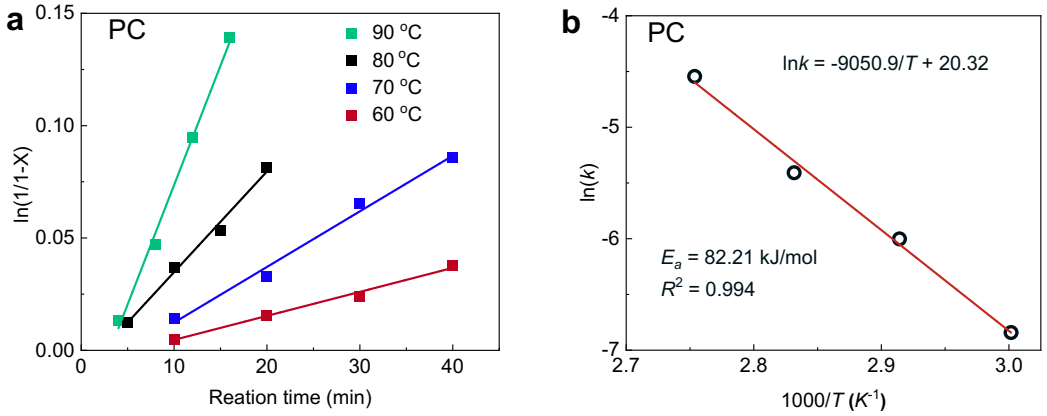

Supplementary Fig. 4 Study on the activation energy of PC methanolysis. (a) Plot of ln[1/(1 − x)] versus time at different temperatures. (b) Arrhenius plots for PC methanolysis. Conditions: [TBDH]Ac (0.5 mmol), PC (0.5 g), MeOH (2 mL), 60–90 °C.

Note:

According to the literature, the PC methanolysis can be regarded as a first-order reaction[1-4]. The reaction equation equations are listed as follows:

$$-\frac{dC_{PC}}{dt} = kC_{PC} \tag{1}$$

$$C_{PC} = C_0\,(1 - x) \tag{2}$$

where k represents the rate constant for PC conversion and C_{PC} represents the PC concentration at a reaction time of t. Where x represents the PC conversion, then as follows:

$$\frac{dx}{dt} = k(1 - x) \tag{3}$$

Integrating eq 3 against time yielded eq 4:

$$\ln[1/(1\text{-}x)] = kt \tag{4}$$

Based on the PC conversion at four different temperatures, the plot of ln[1/(1 − x)] versus the time obtained was linear, as shown in Fig. S4a.

The activation energy for the PC methanolysis was calculated using the Arrhenius equations (eq 5 and eq 6), where A is the pre-exponential factor (h^{-1}), E_a is the activation

energy (kJ mol^{-1}), T is the absolute temperature (K), and R is the universal gas constant (8.314 J mol^{-1} K^{-1}):

$$k = Ae^{-E_a/(RT)} \tag{5}$$

$$\ln k = \ln A - E_a/(RT) \tag{6}$$

Based on the relationship of rate constant k and temperature, Fig. S4b gave a linear correlation of ln k to the reciprocal of temperature ($1/T$).

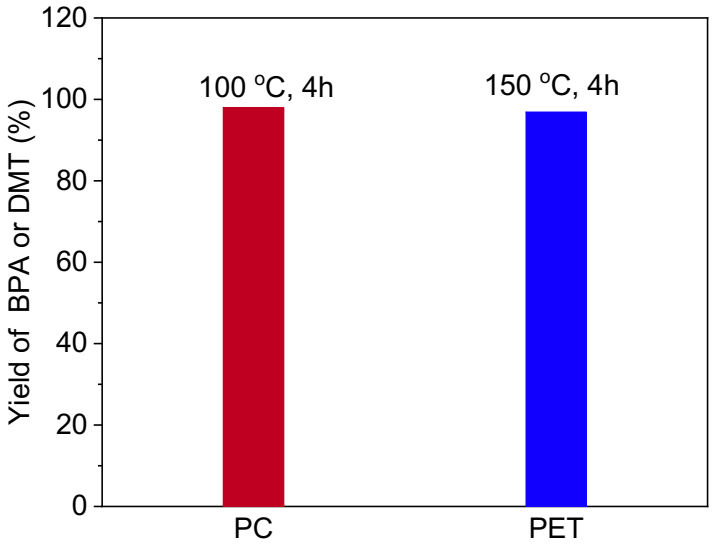

Supplementary Fig. 5 Catalytic methanolysis of PC and PET. Condition: catalyst (0.25 mmol), plastics (0.5 g) and MeOH (2 mL).

Note:

Reaction equation:

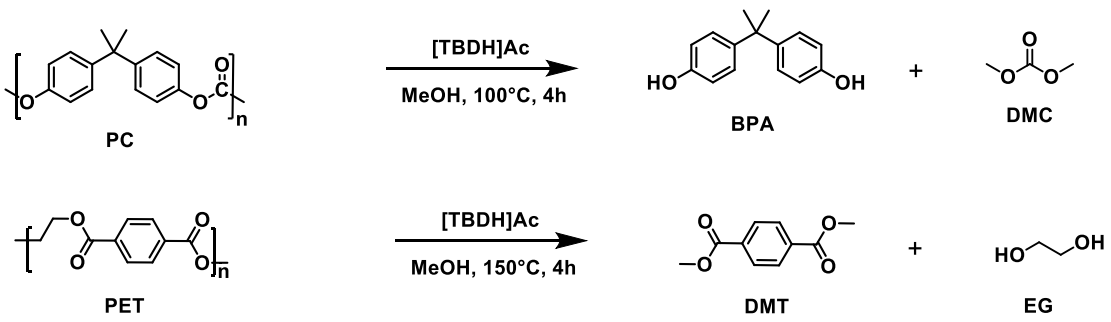

Reaction equipment: A 20 mL 316L stainless-steel autoclave with magnetic stirring. The working pressure is 3.2 atm at 100 °C and the working pressure is 13.5 atm at 150 °C.

Input form: Plastic powder: 0.5 g

Anhydrous methanol (99.9%, Adamas) 4 mL

[TBDH]Ac (0.25 mmol)

Reaction conditions: Reaction temperature: 100 ºC (PC), 150 ºC (PET)

Reaction time: 4 hours

Stirring rate: 500 rpm

Post-processing: At the end of the reaction, the obtained mixture was filtered and washed with methanol to obtain the residual plastics. Then, the residual plastic powder was washed, dried at 70 °C for 12 h, and weighed of plastics powder to calculate the conversion. To quantify DMC or EG, methanol with the products was quantitatively volumized in a 25 ml volumetric flask. The DMC and EG were quantified using external standard methods. The above solvents were concentrated, and the residue was extracted with ethyl acetate and deionized water. The monomers (r-BPA, r-DMT) could be obtained from the organic phase by rotary evaporation and the mass of the products was recorded. The purity of the monomers was analyzed by ^{1}H NMR.

Analysis of DMC and EG:

DMC: Gas chromatography (GC) analysis was recorded on a gas chromatograph (Agilent 7820) equipped with a capillary column (HP-5, 30 m × 320 μm × 0.25 μm) using a flame ionization

detector with a flow rate of 1 mL min^{-1} using the following method: the oven temperature was held at 50 °C for 5 min and then increased linearly to 250 °C over 20 min with a final hold of 5 min.

EG: Ethylene glycol content was detected on Shimadzu (LC-2050) high-performance liquid chromatography (HPLC) equipped with a UV detector and a liquid chromatography column Aminex® HPX-87H. The mobile phase was 8mM H_2SO_4 solution at 35°C with a flow rate of 0.6 mL·min^{-1}. Operation method: equal degree operation for 20 minutes.

Experimental result:

Polymers	*T* (°C)	Time (h)	Conversion (%)	BPA yield (%)[a]	DMC yield (%)[a]
PC	100	4	99	97.3 ± 1.0	95.3 ± 10.0
Polymers	*T* (°C)	Time (h)	Conversion (%)	DMT yield (%)[a]	EG yield (%)[a]
PET	150	4	99	98.7 ± 0.5	93.0 ± 1.8

[a] Error bars indicate standard deviation calculated from three replicate experiments.

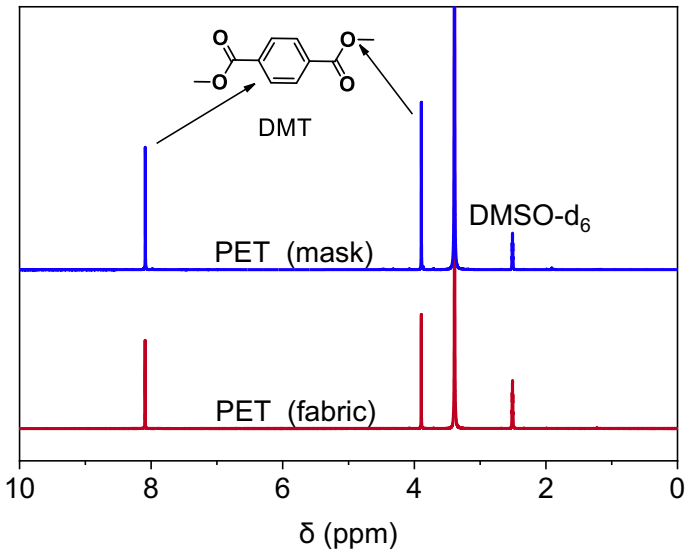

Supplementary Fig. 6 ^{1}H NMR spectra of r-DMT recycled from PET methanolysis (DMSO-d_6, 400 MHz).

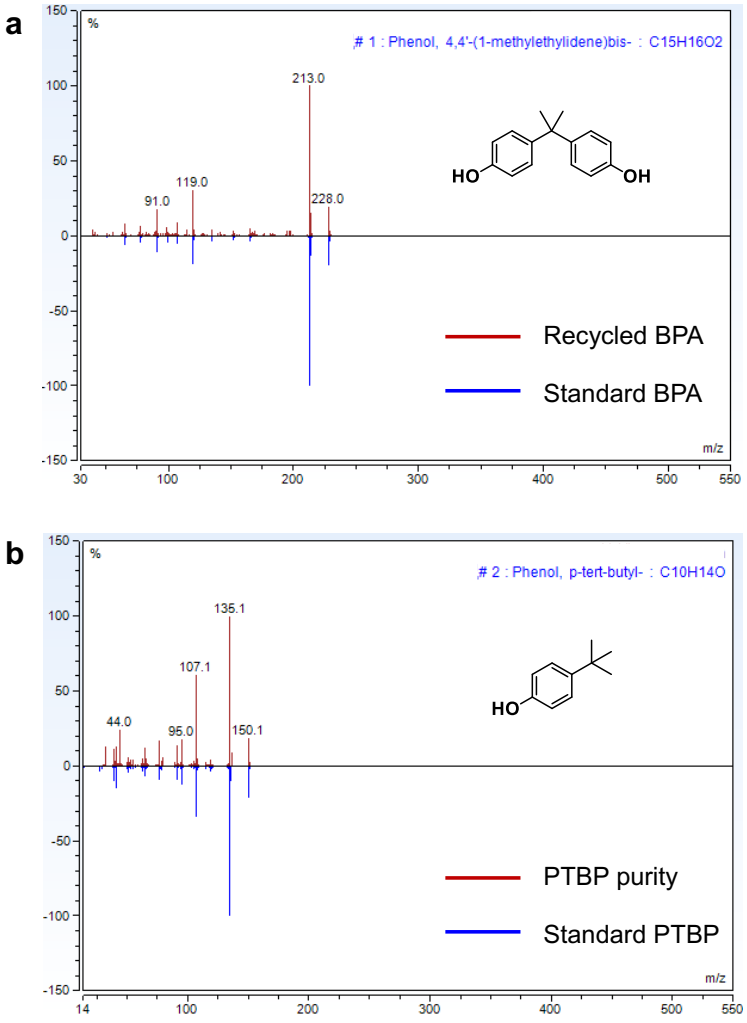

Supplementary Fig. 7 Mass spectrum of BPA and p-tert-butylphenol (PTBP). (a) recycled BPA and standard BPA. (b) PTBP in recycled BPA and standard PTBP.

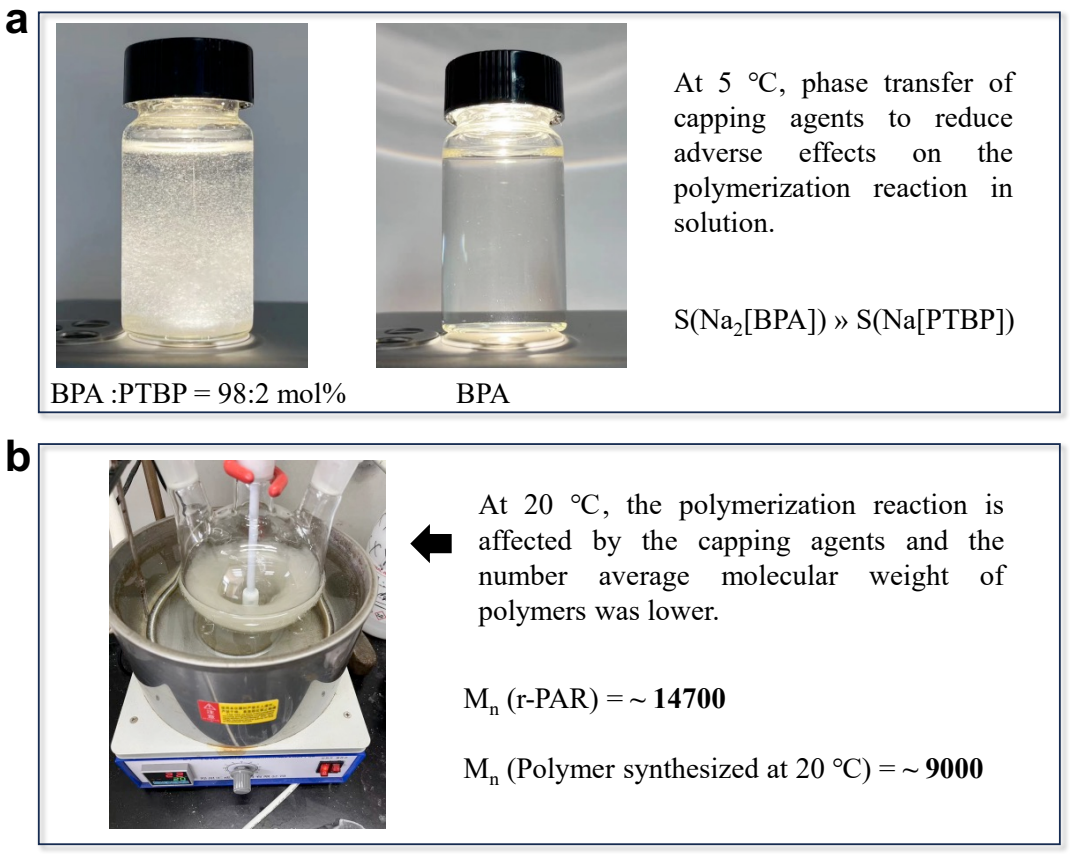

Supplementary Fig. 8 Images of compound solubility (BPA vs PTBP) and uncontrolled temperature polymerization. (a) Solubility of bisphenol A (BPA) and p-tert-butylphenol (PTBP) in reaction solutions at 5 °C (including CH_2Cl_2, H_2O, NaOH). (b) Photographs of polymerization experiments in the absence of variable temperature control.

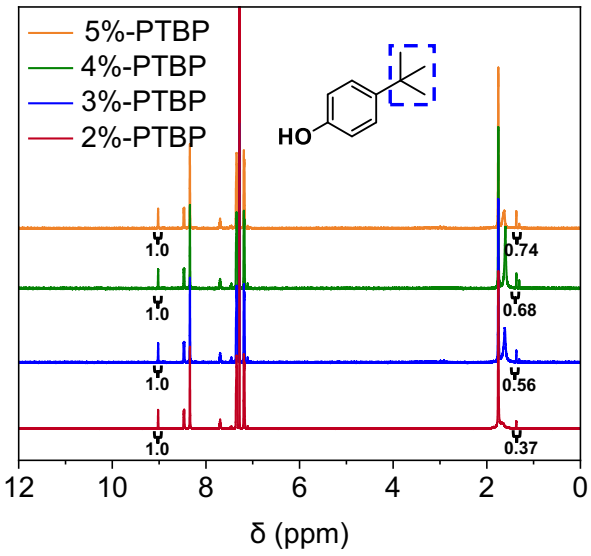

Supplementary Fig. 9 The ^{1}H NMR spectra of PAR with different end-capping agents of PTBP (2-5%) in $CDCl_3$. (TPC+IPC): BPA= 1:0.975; the content of PTBP is in the range of 2-5%.

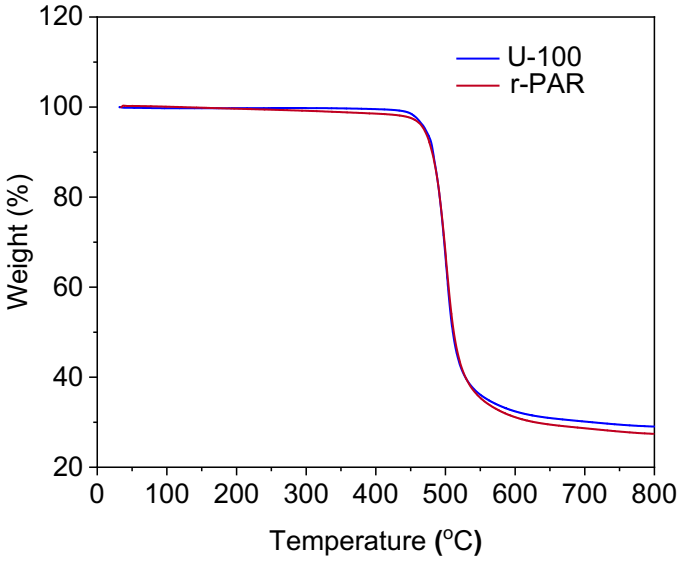

Supplementary Fig. 10 TGA curves of r-PAR and control sample U-100 at a heating rate of 10 °C min^{-1} in N_2 atmosphere.

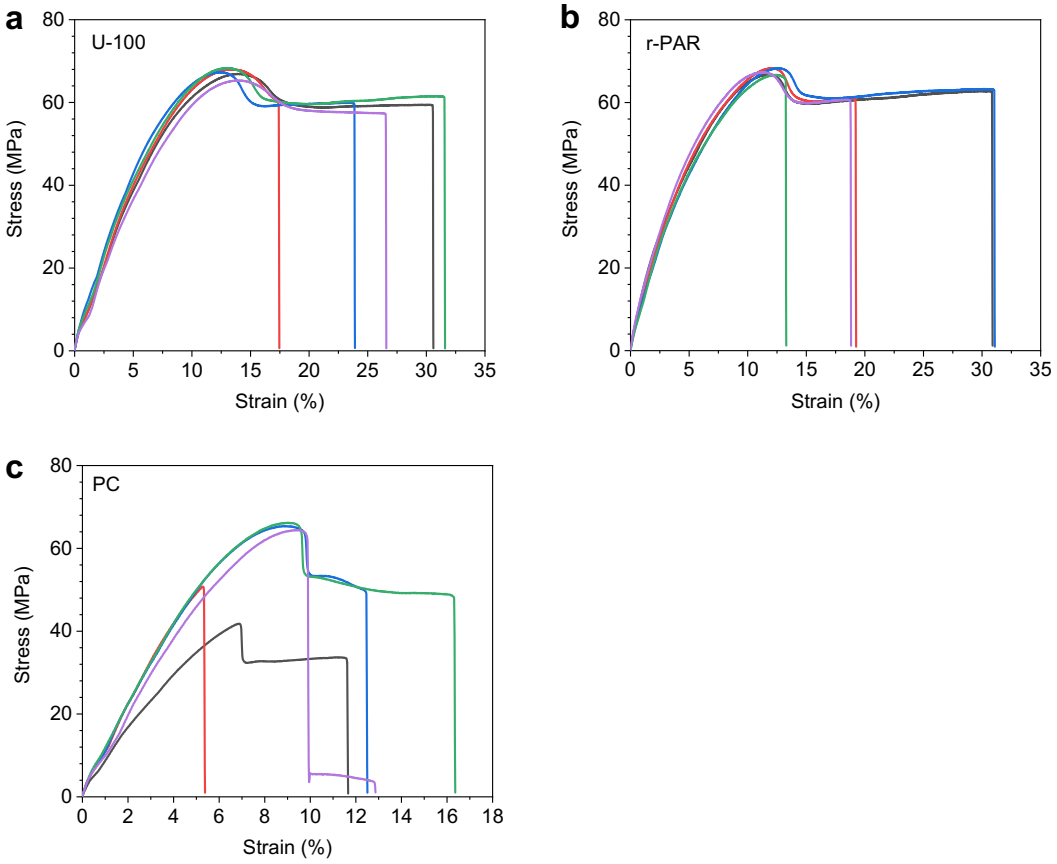

Supplementary Fig. 11 Stress–strain curves of (a) U-100, (b) r-PAR, (c) PC. For accuracy, each value obtained from the average results of 5 specimens

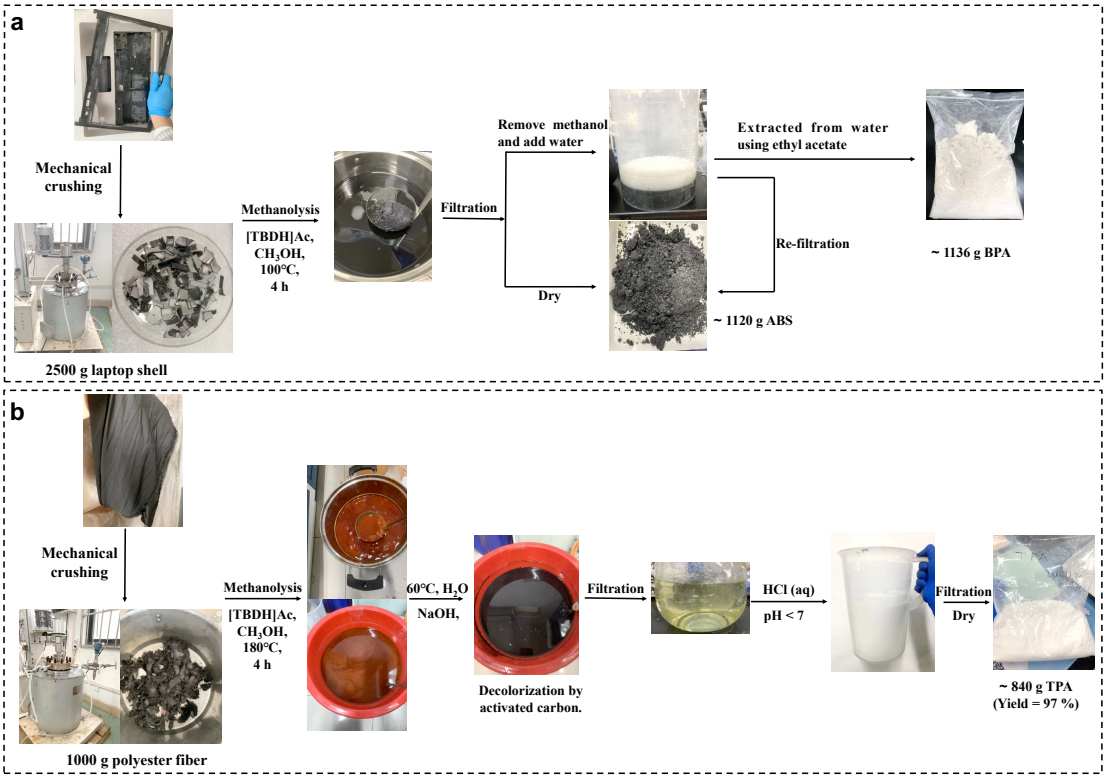

Supplementary Fig. 12 The process of kilogram-gram scale experiments of wastepolymers methanolysis (10 L high-pressure reactor). (a) Laptop shell. (b) Polyester fiber.

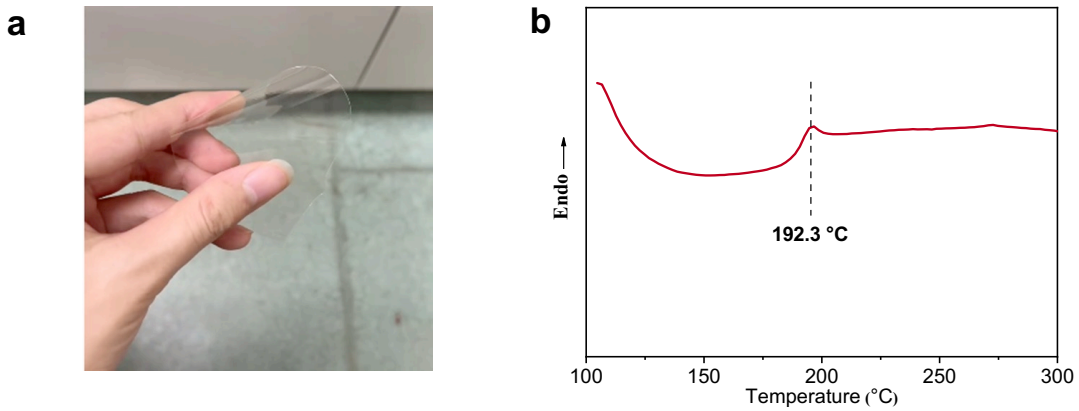

Supplementary Fig. 13 (a) The photograph of r-PAR-CD film (thickness: ~200 μm) hot-pressed at 280 °C. (b) DSC curve of r-PAR-CD.

Note: The r-PAR-CD film was produced as following procedure: 80.0 g of CDs was degraded and 69.5 g of r-BPA-CD was recovered (yield: 96%); Subsequently, the r-BPA-CD (22.8 g, 0.1 mol) was polymerized with TPC (10.2 g, 0.05 mol)/IPC (10.2 g, 0.05 mol) to yield r-PAR-CD film materials using the same method for r-PAR from laptop shells.

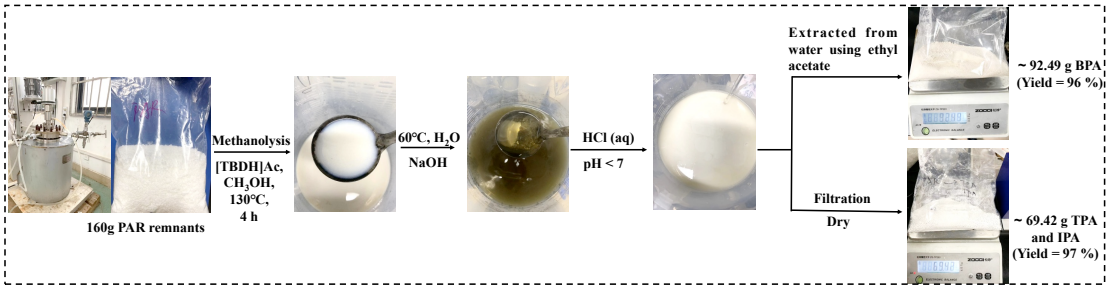

Supplementary Fig. 14 The large-scale experiments of PAR methanolysis. Note: To obtain monomers for PAR synthesis, further treatment of DMT is required. The r-DMT and r-DMI produced by methanolysis were hydrolyzed to TPA and IPA. The TPA and IPA could be further chlorinated to TPC and IPC.

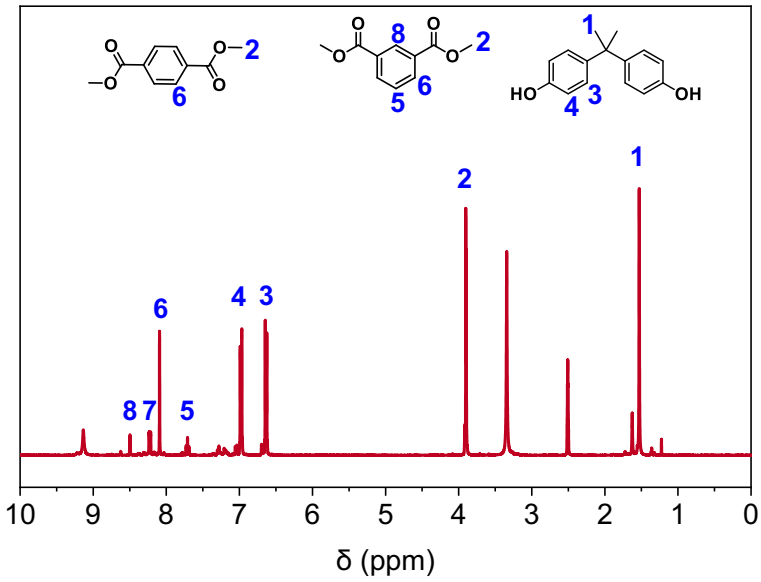

Supplementary Fig. 15 ^{1}H NMR spectra of products recycled from PAR methanolysis (DMSO-d_6, 400 MHz).

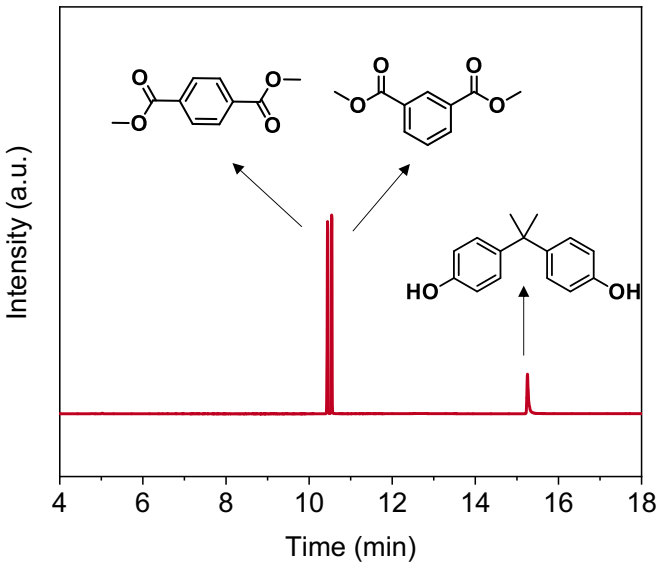

Supplementary Fig. 16 The GC-MS analysis of products recycled from PAR methanolysis.

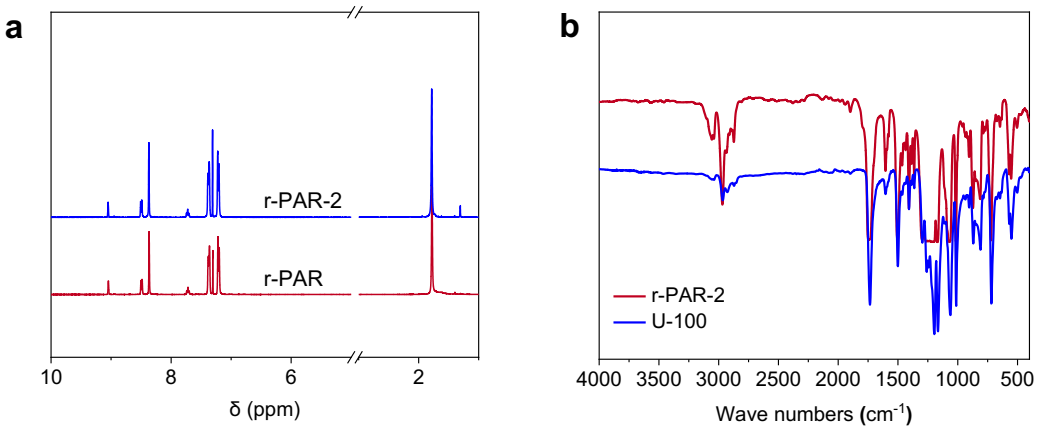

Supplementary Fig. 17 Characterization of r-PAR-2 and U-100. (a) ^{1}H NMR spectra of r-PAR and r-PAR-2 ($CDCl_3$, 400 MHz). (b) The FT-IR spectra of r-PAR-2 and U-100.

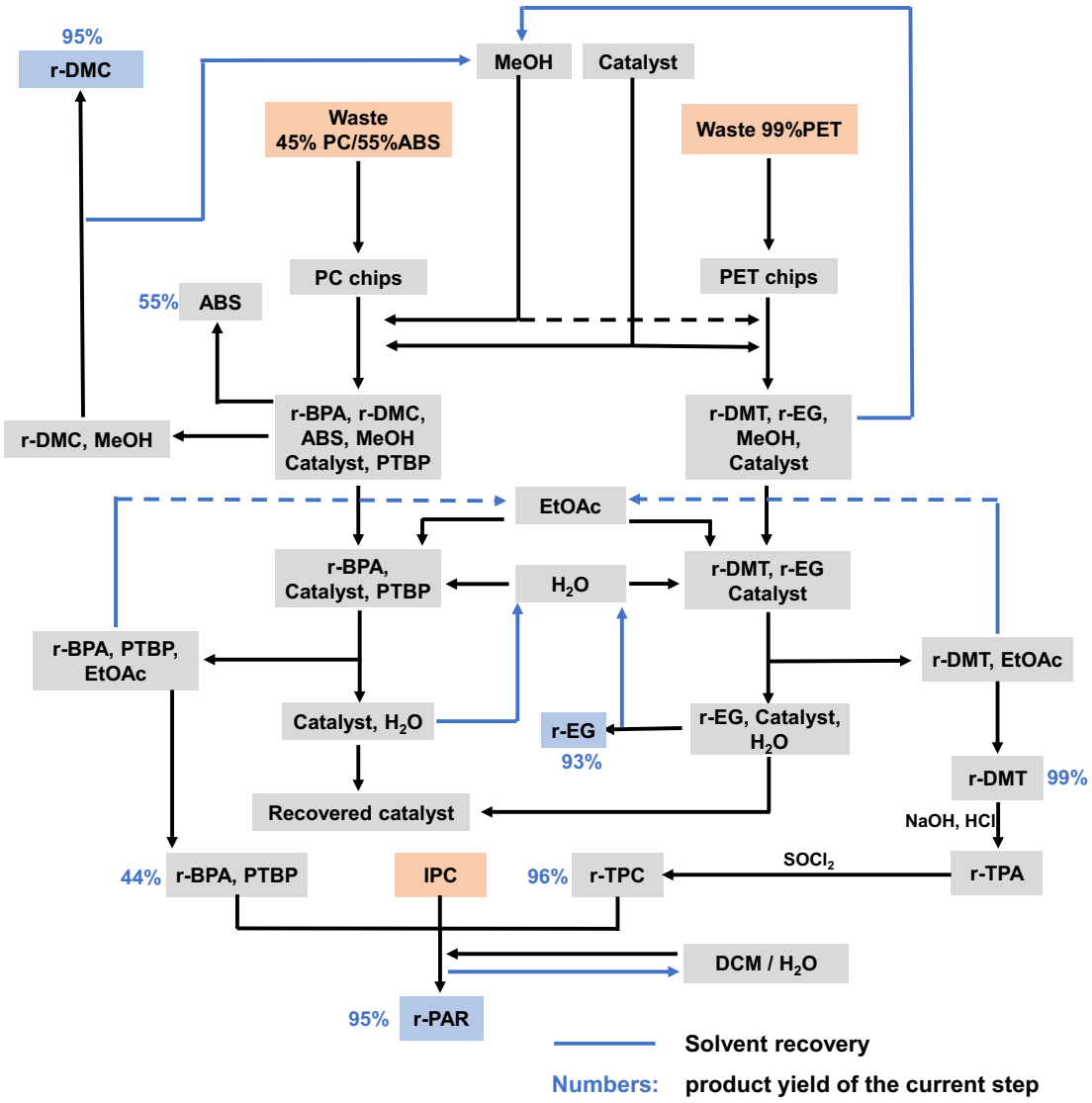

Supplementary Fig. 18 Detailed process of co-upcycling of waste PC and PET to high-performance special engineering plastics- polyarylates. The route is used for LCA calculation.

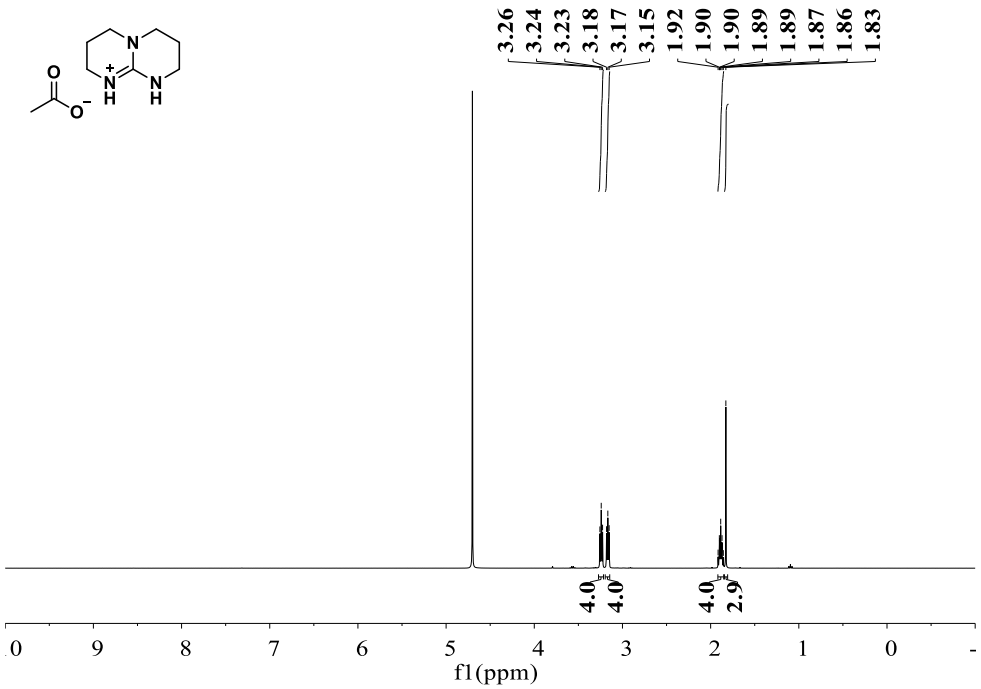

Supplementary Fig. 19 ^{1}H NMR spectrum of [TBDH]Ac. ^{1}H NMR (400 MHz, D_2O) δ 3.33 (t, J = 6.0 Hz, 4H), 3.29 – 3.22 (m, 4H), 1.97 (p, J = 5.9 Hz, 4H), 1.92 (s, 3H).

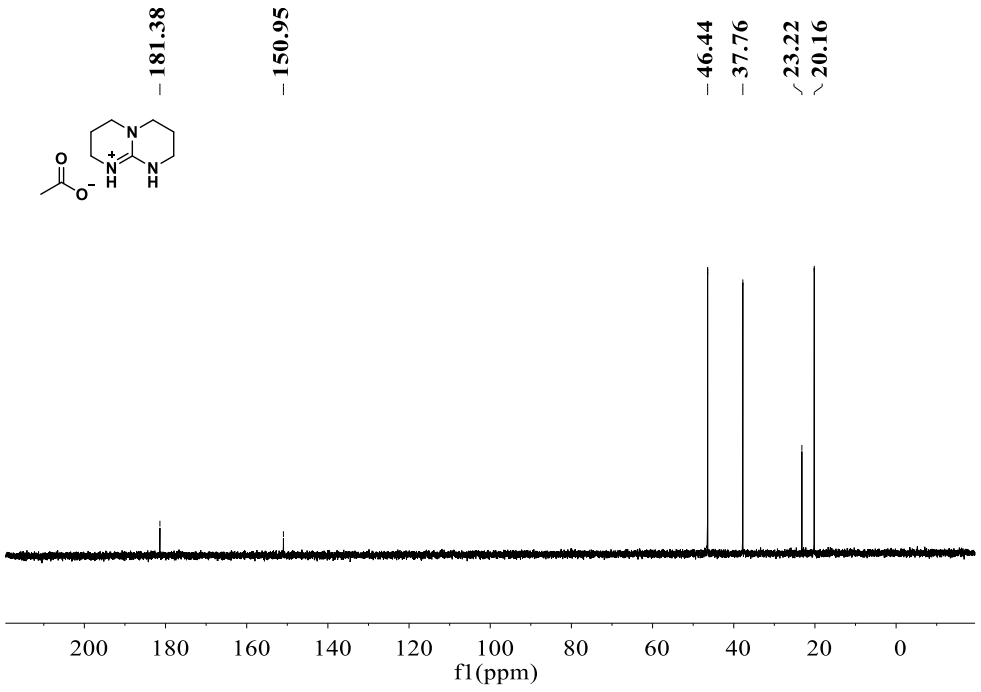

Supplementary Fig. 20 ^{13}C NMR spectrum of [TBDH]Ac. ^{13}C NMR (101 MHz, D_2O) δ 181.38, 150.95, 46.44, 37.76, 23.22, 20.16.

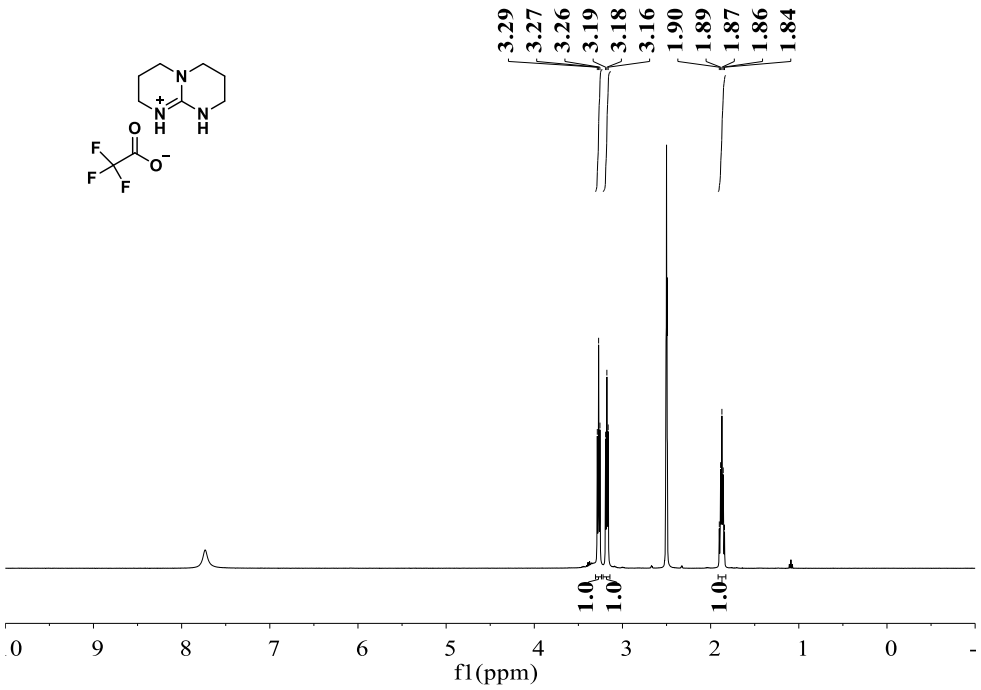

Supplementary Fig. 21 ^{1}H NMR spectrum of [TBDH]TFA. ^{1}H NMR (400 MHz, DMSO-d_6) δ 3.27 (t, J = 6.0 Hz, 1H), 3.22 – 3.14 (m, 1H), 1.87 (p, J = 5.9 Hz, 1H).

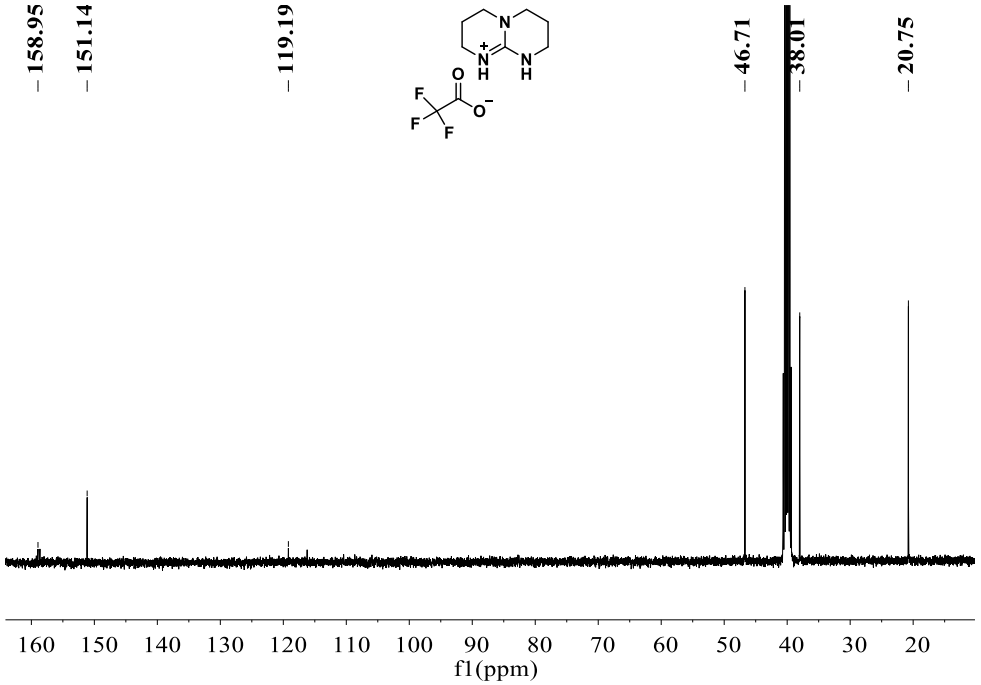

Supplementary Fig. 22 ^{13}C NMR spectrum of [TBD]TFA. ^{13}C NMR (101 MHz, DMSO-d_6) δ 158.95, 151.14, 119.19, 46.71, 38.01, 20.75.

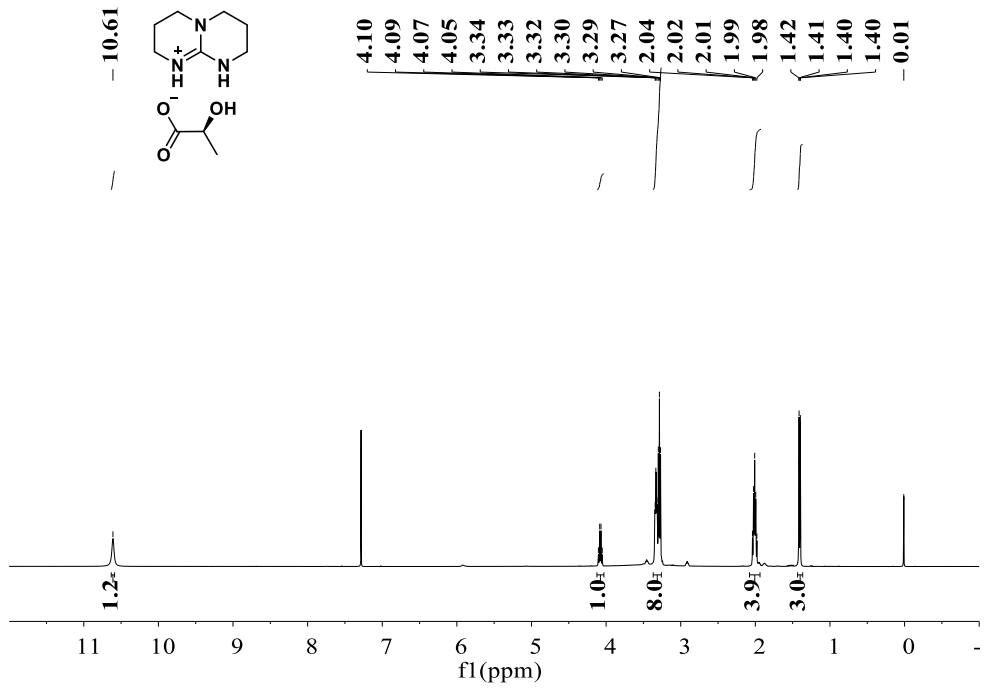

Supplementary Fig. 23 ^{1}H NMR spectrum of [TBDH]LA. ^{1}H NMR (400 MHz, $CDCl_3$) δ 10.61 (s, 1H), 4.08 (q, J = 6.9 Hz, 1H), 3.36 – 3.25 (m, 8H), 2.01 (p, J = 5.9 Hz, 4H), 1.41 (dd, J = 6.9, 1.0 Hz, 3H).

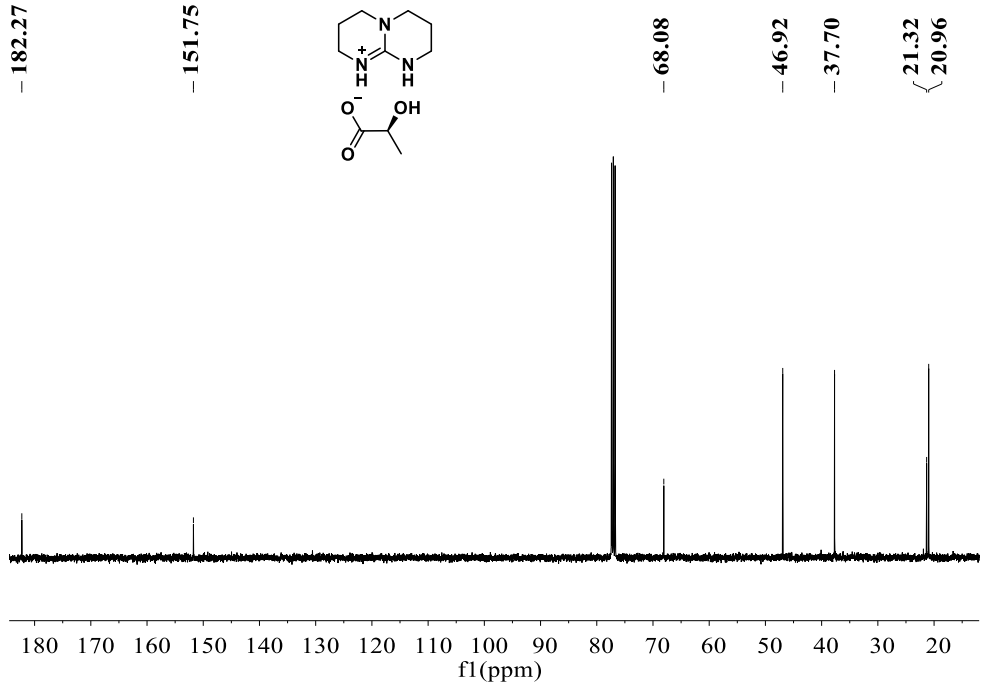

Supplementary Fig. 24 ^{13}C NMR spectrum of [TBDH]LA. ^{13}C NMR (101 MHz, $CDCl_3$) δ 182.27, 151.75, 68.08, 46.92, 37.70, 21.32, 20.96.

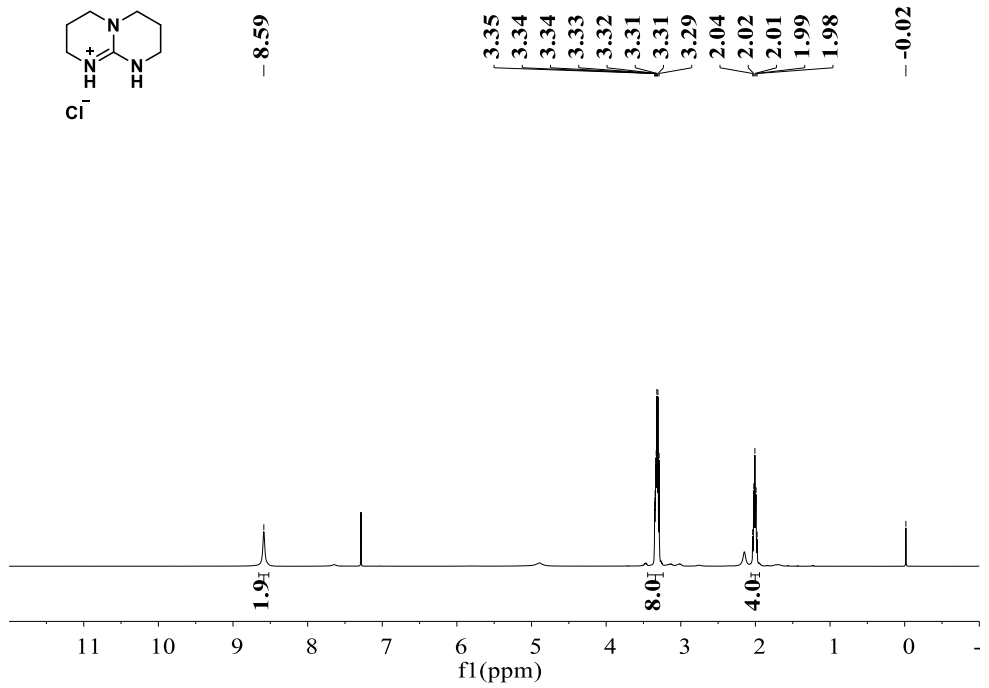

Supplementary Fig. 25 ^{1}H NMR spectrum of [TBDH]Cl. ^{1}H NMR (400 MHz, $CDCl_3$) δ 3.32 (ddd, J = 12.0, 7.5, 4.6 Hz, 8H), 2.01 (p, J = 5.9 Hz, 4H).

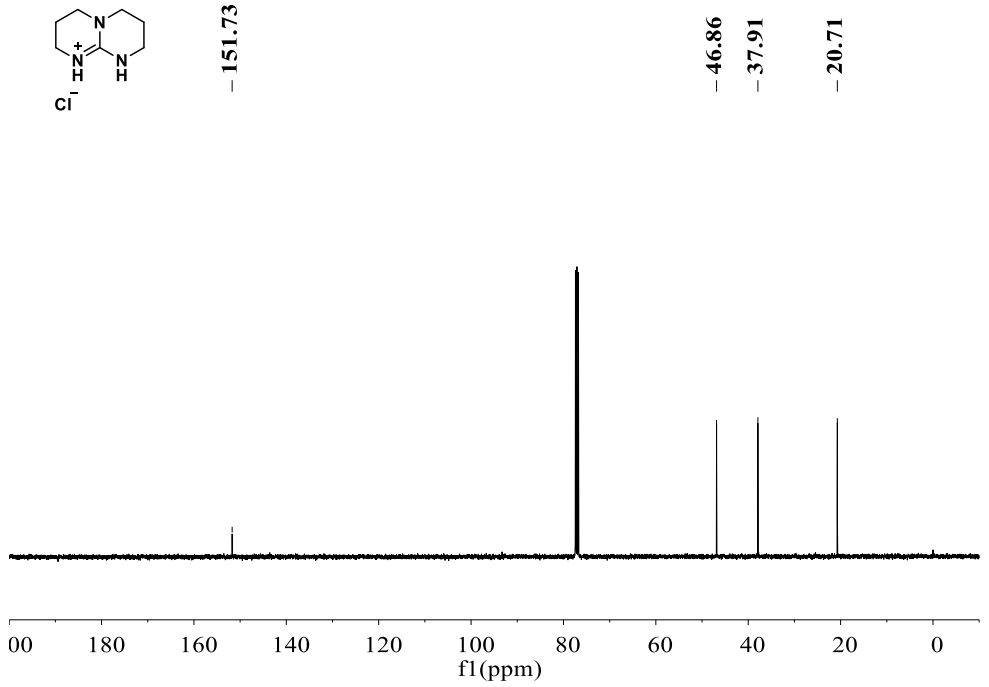

Supplementary Fig. 26 ^{1}H NMR spectrum of [TBDH]Cl. ^{13}C NMR (101 MHz, $CDCl_3$) δ 151.73, 46.86, 37.91, 20.71.

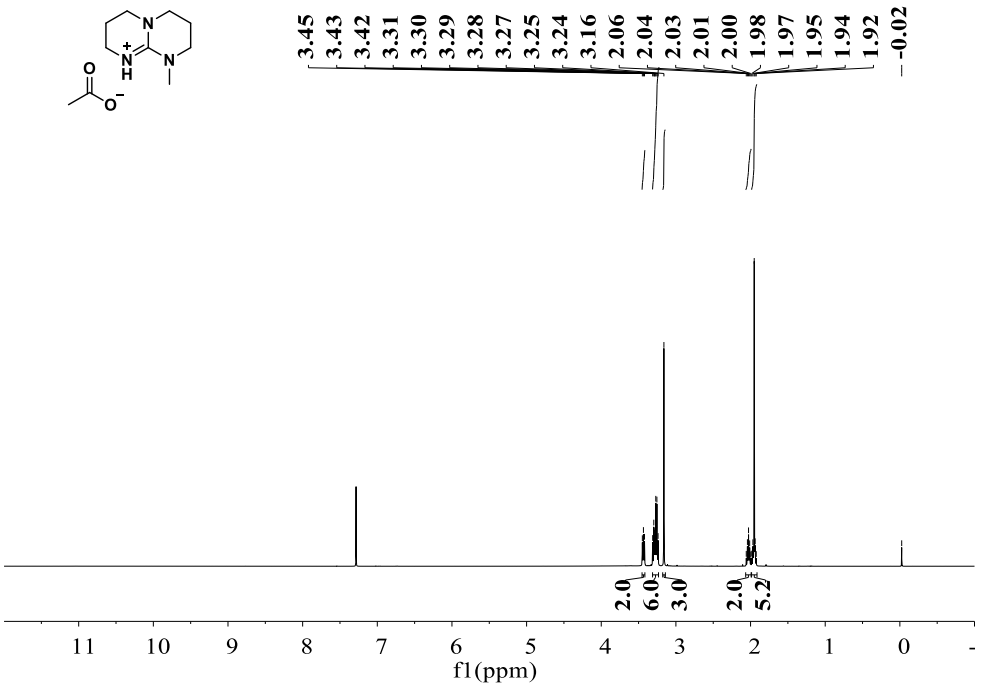

Supplementary Fig. 27 ^{1}H NMR spectrum of [MTBDH]Ac. ^{1}H NMR (400 MHz, $CDCl_3$) δ 3.32 (ddd, J = 12.0, 7.5, 4.6 Hz, 8H), 2.01 (p, J = 5.9 Hz, 4H).

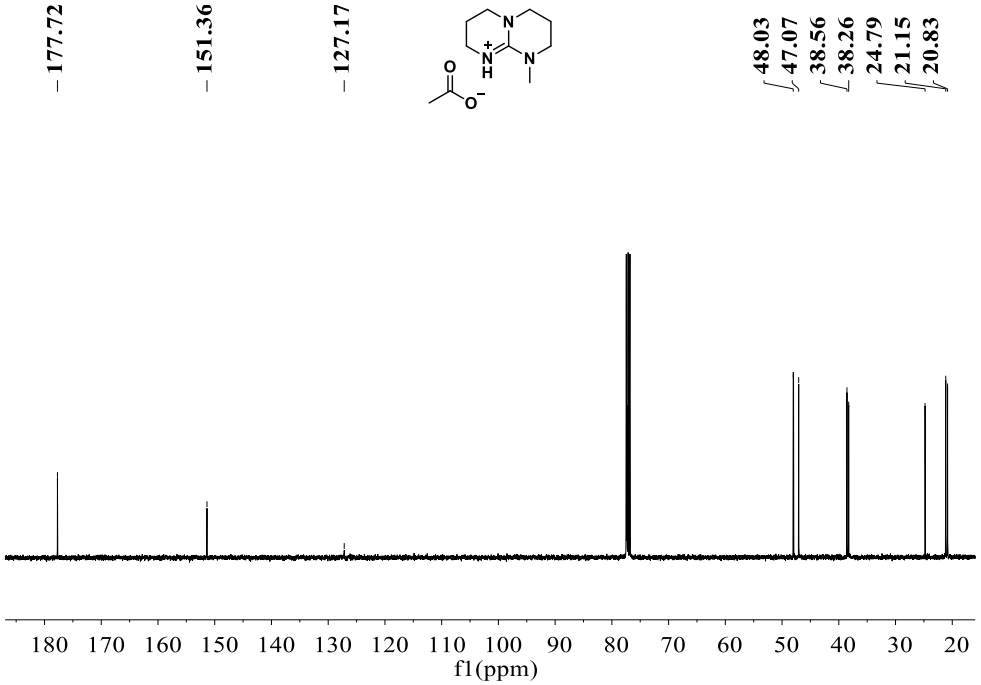

Supplementary Fig. 28 ^{1}H NMR spectrum of [MTBDH]Ac. ^{1}H NMR (400 MHz, $CDCl_3$) δ 3.32 (ddd, J = 12.0, 7.5, 4.6 Hz, 8H), 2.01 (p, J = 5.9 Hz, 4H).

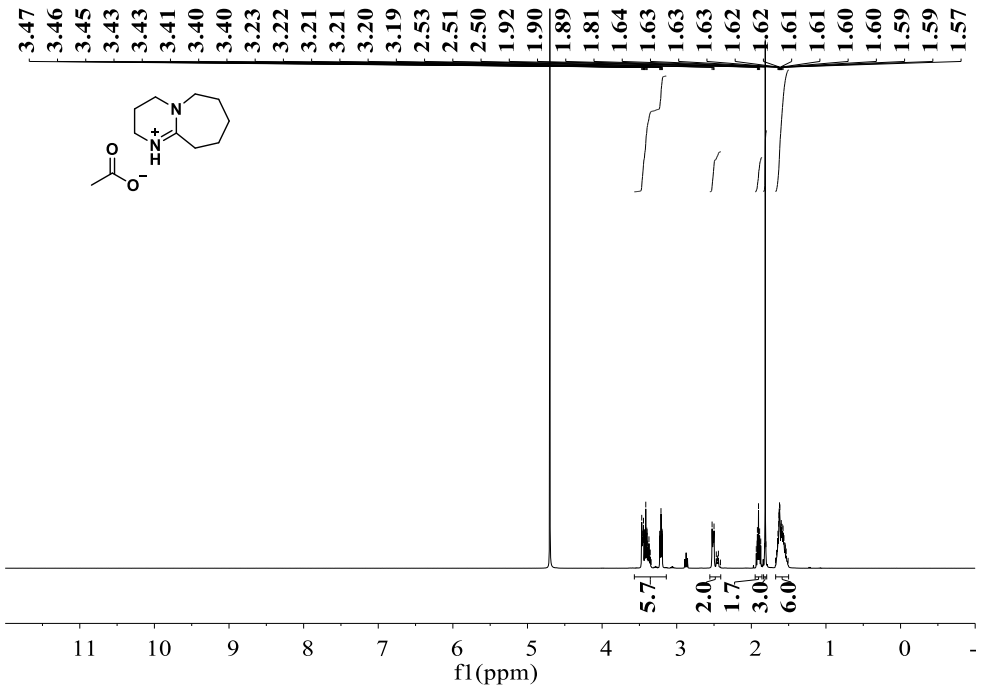

Supplementary Fig. 29 ^{1}H NMR spectrum of [DBUH]Ac. ^{1}H NMR (400 MHz, DMSO-d_6) δ 3.57 – 3.14 (m, 6H), 2.56 – 2.41 (m, 2H), 1.95 – 1.86 (m, 2H), 1.81 (s, 3H), 1.67 – 1.50 (m, 6H).

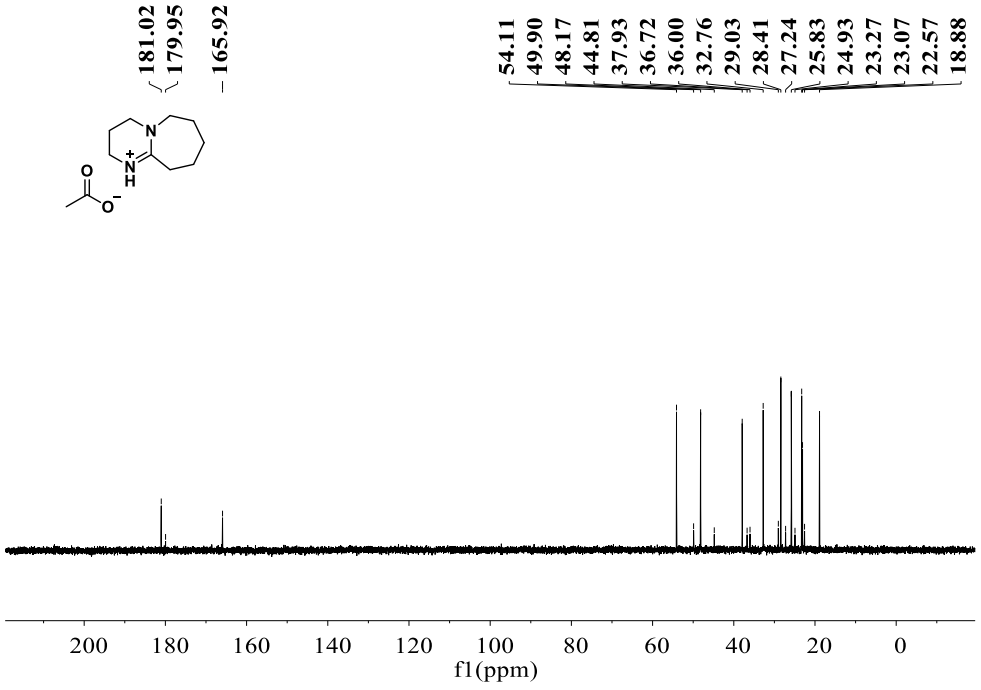

Supplementary Fig. 30 ^{1}H NMR spectrum of [DBUH]Ac. ^{13}C NMR (101 MHz, D_2O) δ 181.02, 179.95, 165.92, 54.11, 49.90, 48.17, 44.81, 37.93, 36.72, 36.00, 32.76, 29.03, 28.41, 27.24, 25.83, 24.93, 23.27, 23.07, 22.57, 18.88.

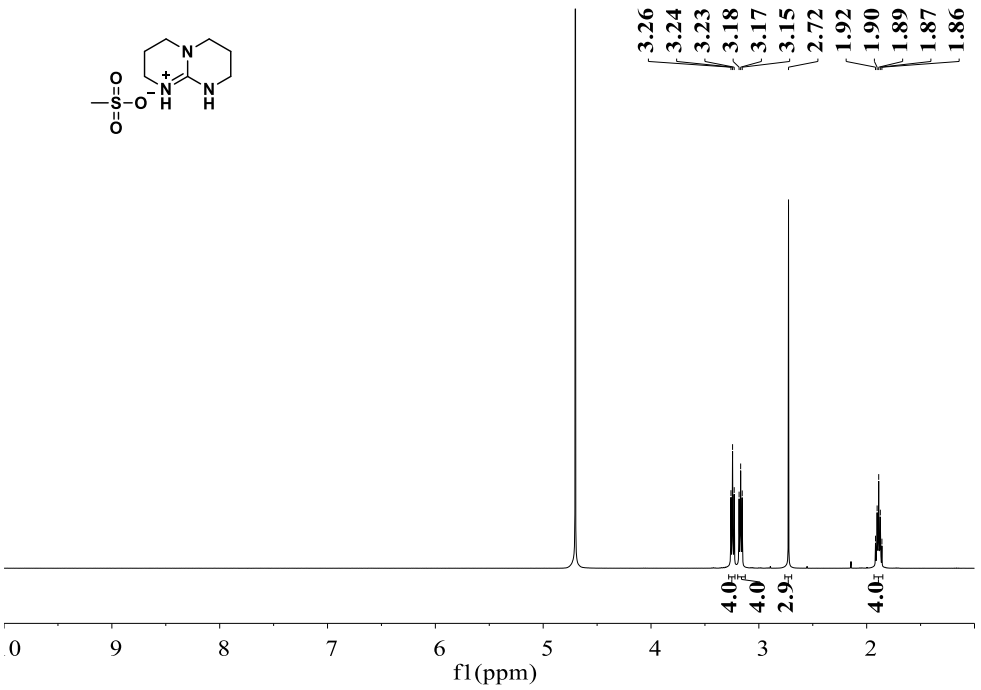

Supplementary Fig. 31 ^{1}H NMR spectrum of [TBDH]MSA. ^{1}H NMR (400 MHz, D_2O) δ 3.24 (t, J = 6.0 Hz, 4H), 3.20 – 3.13 (m, 4H), 2.72 (s, 3H), 1.89 (p, J = 5.9 Hz, 4H).

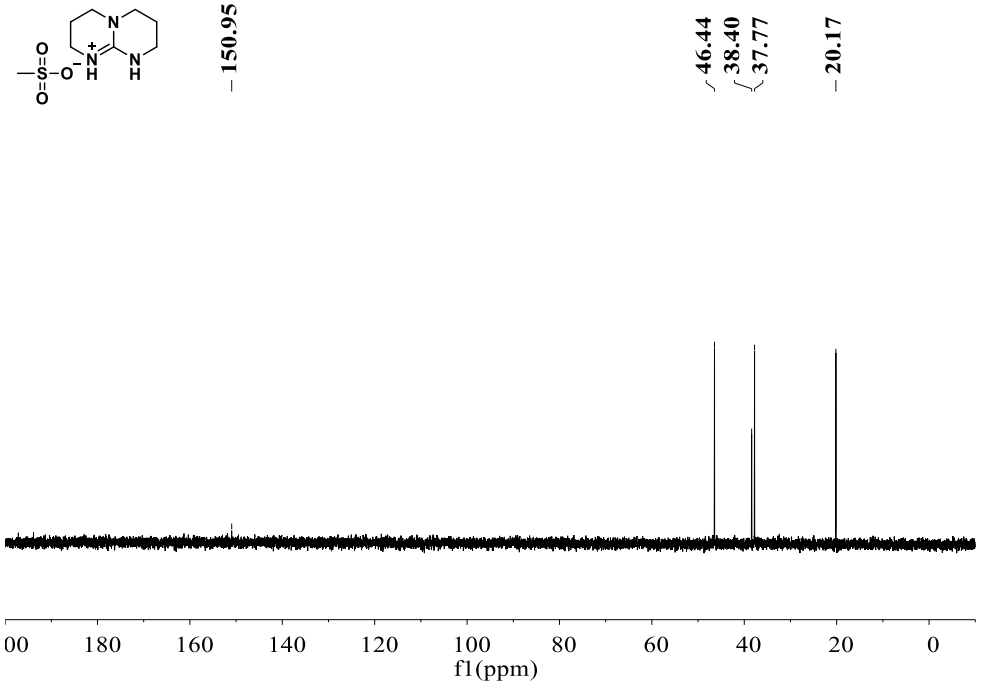

Supplementary Fig. 32 ^{13}C NMR spectrum of [TBDH]MSA. ^{13}C NMR (101 MHz, D_2O) δ 150.95, 46.44, 38.40, 37.77, 20.17.

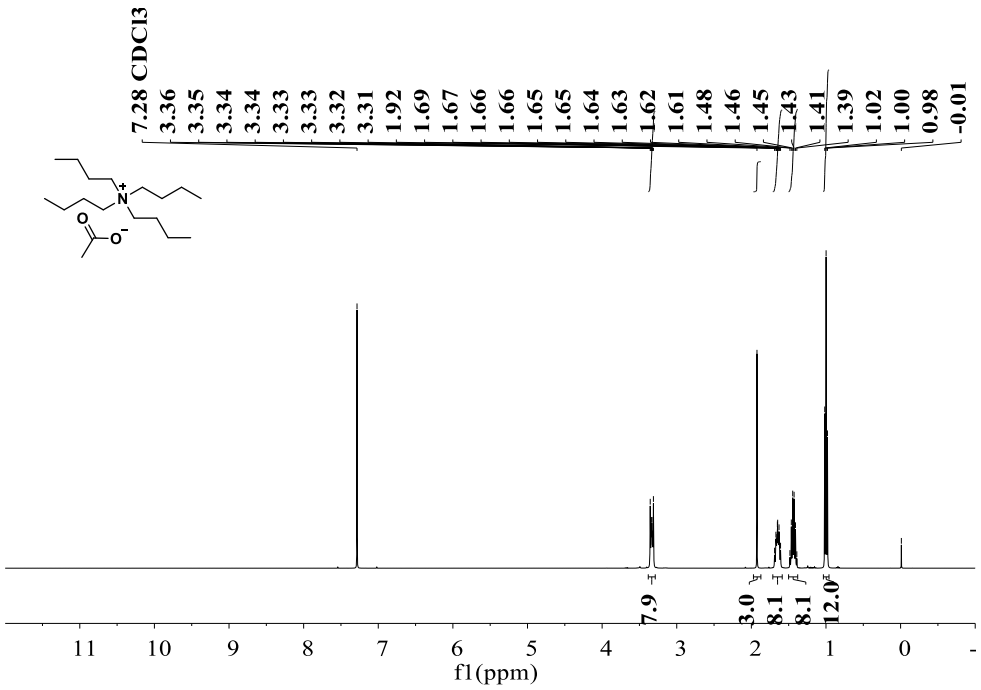

Supplementary Fig. 33 ^{1}H NMR spectrum of [N_{4444}]Ac. ^{1}H NMR (400 MHz, $CDCl_3$) δ 3.38 – 3.29 (m, 8H), 1.92 (s, 3H), 1.65 (dq, J = 11.9, 8.2, 7.7 Hz, 8H), 1.44 (h, J = 7.4 Hz, 8H), 1.00 (t, J = 7.3 Hz, 12H).

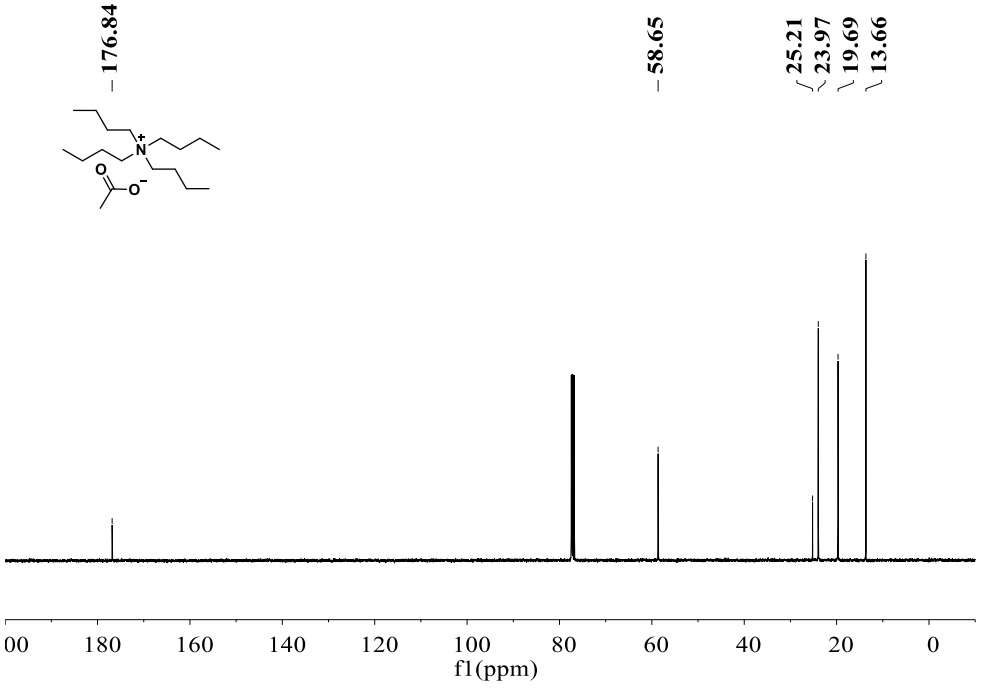

Supplementary Fig. 34 ^{13}C NMR spectrum of [N_{4444}]Ac. ^{13}C NMR (101 MHz, $CDCl_3$) δ 176.84, 58.65, 25.21, 23.97, 19.69, 13.66.

Supplementary Table 1 The molecular weight of PAR with different contents of end-capping agent PTBP.

Sample	M_n (g/mol)	M_w (g/mol)	PDI
PAR-2%PTBP	13879	55594	4.00
PAR-3%PTBP	14471	60580	4.19
PAR-4%PTBP	17752	63813	3.59
PAR-5%PTBP	14770	49153	3.33

Supplementary Table 2 Inherent viscosities, thermal and mechanical properties of r-PAR, control sample U-100 and PC.

Polymers	GPC			Inherent viscosity (dL g^{-1}) [a]	T_g [b] (°C)	$T_{5\%}$ [c] (°C)	Tensile strength (MPa) [e]	Elongation at Break (%) [e]
	M_w	M_n	PDI					
U-100	3.85×10^4	1.83×10^4	2.10	0.55	194.8	473	67.20±1.18	25.95±5.71
r-PAR	4.32×10^4	1.47×10^4	2.94	0.53	192.8	470	67.49±0.77	22.6±7.95
PC [d]	3.00×10^4				143.3		57.73±10.92	11.68±3.99

[a] measured in polymer solution of 0.5 g dL^{-1} in NMP at 30 °C; [b] Tested at DSC with a heating rate of 10 °C min^{-1}, [c] Tested at TGA with a heating rate of 10 °C min^{-1}, [d] PC (Mitsubishi), Grades: H-4000. [e] Error bars indicate standard deviation calculated from replicate experiments.

Supplementary Table 3 The operational parameters of kilogram scale reaction.

Polymers	Reaction time (h)	Reaction temperature (°C)	Heating time (min)	Real-time temperature(°C)	System pressure (MPa)	Stirring rate (rpm)	Stirring form
PC	4	100	0	28.5	0.0	265	Mechanical mixing
			20	30.0	0.0		
			40	40.8	0.0		
			60	76.5	0.1		
			70	100.1	0.3		
			310	102.2	0.3		
PET	4	150	0	28.5	0.0	265	Mechanical mixing
			20	32.2	0.0		
			40	45.5	0.0		
			60	83.1	0.2		
			80	105.2	0.4		
			100	128.8	0.9		
			115	149.2	1.41		
			355	150.8	1.40		

Supplementary Note: Life-cycle assessment

The system boundary of LCA was set as "cradle to gate" (the collection and transportation of waste plastic, the whole processes of depolymerization of waste plastic, the production of chemical raw materials, the production or re-polymerization of PC film, amorphous PET resin in forms of chips, and residual material from PAR production.) because the subsequent use and disposal of various products vary widely. The data on the collection and transportation of waste plastics refer to the database of existing process data, i.e. PET production, mechanical recycling of PET, etc. For analysis, our material balance and energy balance were derived from process data of PAR production in the company. Other process dates were derived from the actual experimental results of commodity polymers methanolysis. The LCA analysis followed the ISO standard series 14040 and 14067. Data used to build the life-cycle inventory were collected from scale-up experimental and the commercial database Ecoinvent 3.7. The mass allocation method was used to distribute the carbon emissions among the chemicals produced within the system. The distribution of electricity used by LCA is 52% thermo- electricity, 45% hydroelectricity, 1.8% wind electricity, and 1.2% other electricity. This data comes from the China Electric Power Statistical Yearbook 2020.

According to ISO 14040/44, LCA needs to be allocated in several cases. For example, in the case of recycled waste material from a product that has been discarded after use and enters the production system of a new product, a rational recycling method is required at this stage to calculate the allocation of environmental benefits between the discarded material and the new product. The environmental benefits of recyclable waste are shared over the life cycle of the current product and the next product, as well as retrogressively, citing the "50/50" allocation methodology, which has been discussed and accepted by the PEF association. It distributes the impacts and benefits of recycling equally between producers who use recyclable materials and those who produce recyclable products[5,6].

Recycling process specific information for the distribution of environmental benefits generated by renewable waste goods, the concept of a correction factor for the quality of renewable waste (Q) is introduced to correct the PEF allocation factor (A,

50%). *Q* is corrected using an economic value correction, i.e., the price of the recycled raw material of the product/price of the virgin raw material. It should be noted that when the difference in performance between the recycled product and the virgin product is not significant, no correction is considered necessary, i.e., the correction factor between the recycled product and the virgin product is 1. The environmental benefit allocation factor (*D*) for the final recyclable waste consists of the three parameters *Q*, *A*, and the percentage of waste recycled and recovered (*rp*). The recycling formula is shown below:

$$D = A * Q * rp \tag{7}$$

D: Quality correction factor for recycled waste

A: PEF allocation factor, A = 50%

Q: quality/price correction factor

rp: Recycling recovery rate.

The environmental benefits of waste recycling to society are essentially conserved; if the market recovery rate *rp* is lower, a higher distribution factor *D* means that the waste is more difficult to recycle, and therefore the producer of that waste will be allocated a higher environmental burden.

Supplementary Table 4 Material and energy input-output of virgin PET, functional unit = 1 tonne PC. (Path 1)

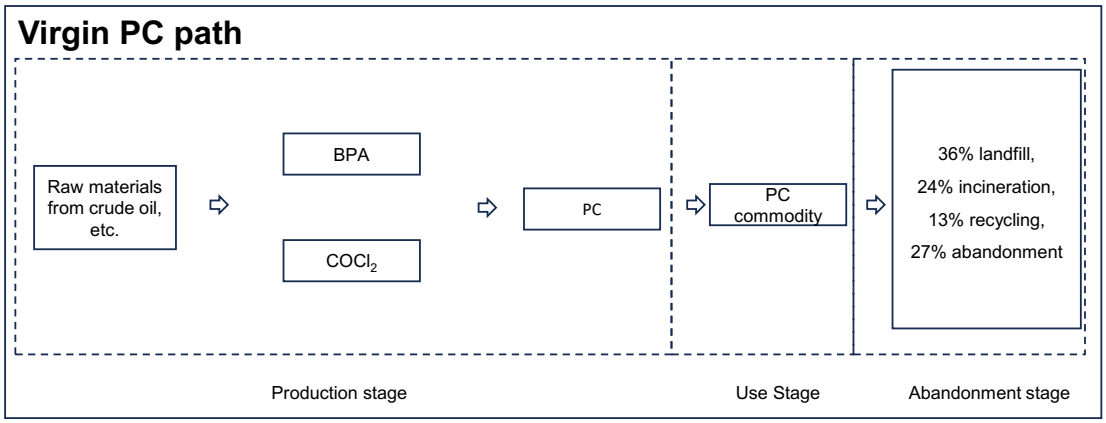

- The regeneration rate (*rp*) of the recycling is assumed to be 97%.

Item	Quantity	Unit
Input:		
Electricity, low voltage	128	kwh
p-tert-butylphenol	0.014	t
Heat (from steam)	1.26	t
BPA	0.87	t
Liquid caustic soda	1.38	t
Hydrochloric acid (31%)	0.192	t
Additives	0.020	t
Liquid chlorine	0.343	t
Dichloromethane	0.5	kg
Stabilizer	1.1	kg
Activated carbon	0.02	kg
Triethylamine (TEA)	0.2	kg
Tap-water	11.8	t
Output:		
PC	1	t
Environmental emissions (Unspecified type, without CO_2)	0.6358	kg

Supplementary Table 5 Material and energy input-output of virgin PET, functional unit = 1 tonne PET. (Path 2)

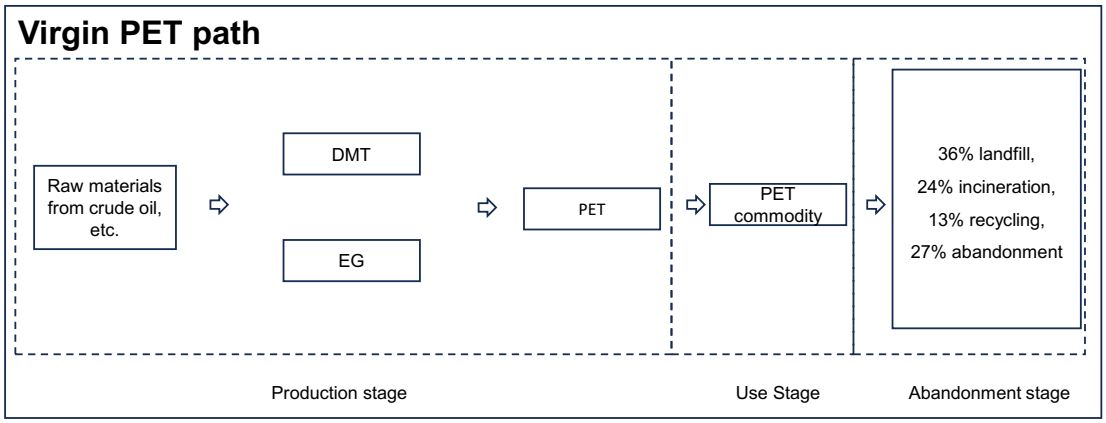

- The regeneration rate (*rp*) of the recycling is assumed to be 97%.

Item	Quantity	Unit
Input:		
Electricity, low voltage	150	kwh
Heat (from steam)	0.2	t
DMT	0.86	t
EG	0.335	t
N_2	15	m^3
TiO_2	3.1	kg
fuel oil	76	kg
Desalted water	0.1	t
Tap-water	0.16	t
Output:		
PET	1	t
Environmental emissions (Unspecified type, without CO_2)	1.363	kg

Supplementary Table 6 Material and energy input-output of virgin PAR, functional unit = 1 tonne PAR. (Path 3)

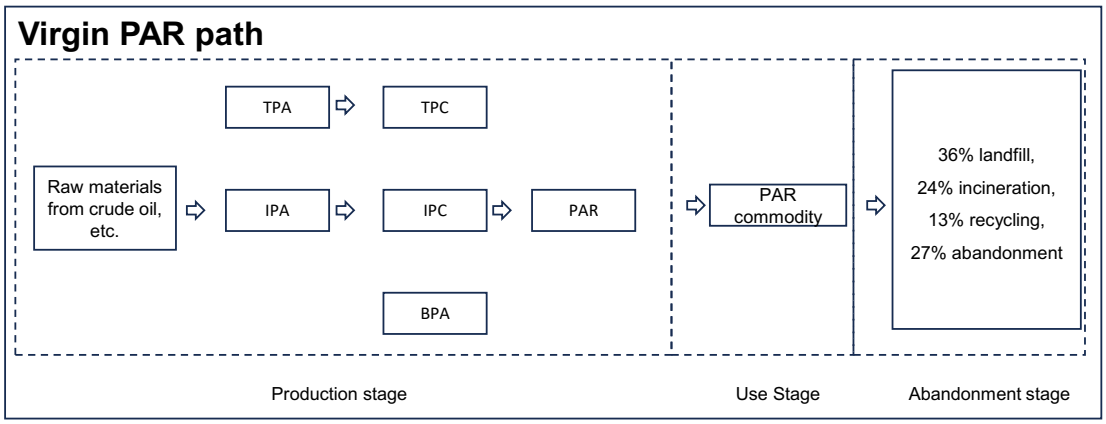

- The regeneration rate (*rp*) of the recycling is assumed to be 97%.

Item	Quantity	Unit
Input:		
Electricity, low voltage	212	kwh
Heat (from steam)	6.2	t
Caustic soda (98%)	0.228	t
Dichloromethane	0.131	t
N_2	20	m^3
Ethanol	4	t
Catalyst	0.1	kg
TPC	0.283	t
IPC	0.283	t
BPA	0.457	t
Desalted water	6	t
Tap-water	3.63	t
Output:		
PAR	1	t

Supplementary Table 7 Material and energy input-output of co-upcycling of waste PC and PET into r-PAR, functional unit = 1 tonne polymer, calculated based on the mass ratio of each chemical. (Case 1)

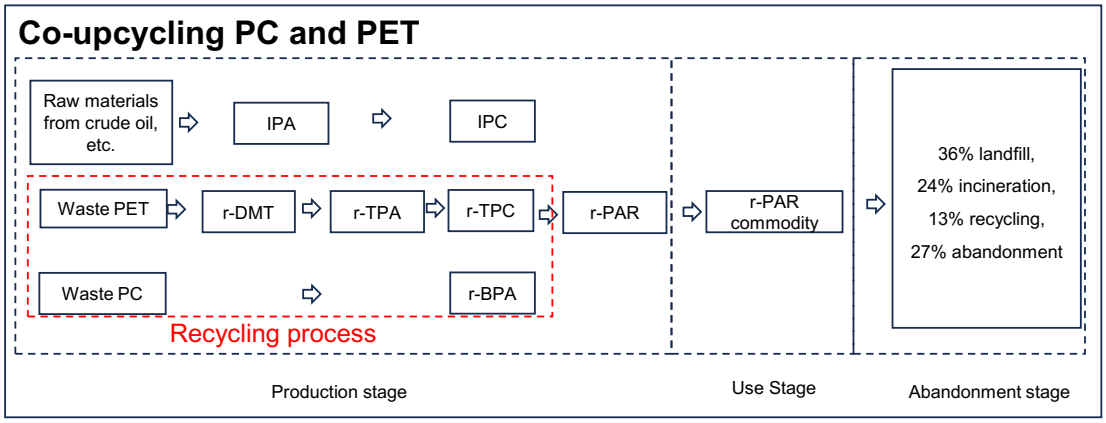

- With raw materials deduction and with recycling deduction
- The regeneration rate (*rp*) of the recycling is assumed to be 96% based on the results of the kilogram-scale experiments. .

Item	Quantity	Unit
Input: waste PET→r-DMT→r-TPA→r-TPC		
waste PET	1	t
Electricity, low voltage	773.9	kwh
Heat (from steam)	4.26	t
Catalyst	10.08	kg
MeOH	333	kg
Desalted water	4	t
Tap-water	3.514	t
N_2	20	m^3
Caustic soda (98%)	0.455	t
Hydrochloric acid (31%)	1	t
Activated carbon	0.01	t
Sulfuric acid	18.76	kg
Dichlorosulfoxide	1.186	t
Output:		
r-TPC	0.98	t
EG	0.306	t
NaCl	0.676	t
Na_2SO_3 (30%)	92.5	kg

Item	Quantity	Unit
Input: waste PC→r-BPA		
Waste PC	1	t
Electricity, low voltage	205	Kwh
Heat (from steam)	0.4	t
Catalyst	10	kg
MeOH	251.68	kg
Desalted water	0.5	t
Tap-water	0.1	t
Output:		
r-BPA	0.89	t
DMC	0.354	t
Waste water	0.5	t

Item	Quantity	Unit
Input: r-PAR production		
Electricity, low voltage	212	kwh
Heat (from steam)	6.2	t
Caustic soda (98%)	0.228	t
Dichloromethane	0.131	t
N_2	20	m^3
Ethanol	4	t
Catalyst	0.1	kg
r-TPC (from waste PET)	0.283	t
IPC	0.283	t
r-BPA (from waste PC)	0.457	t
Desalted water	6	t
Tap-water	3.63	t
Output:		
r-PAR	1	t

Supplementary Table 8 Material and energy input-output of closed-loop recycling of PAR, functional unit = 1 tonne PAR, calculated based on the mass ratio of each chemical. (Case 2)

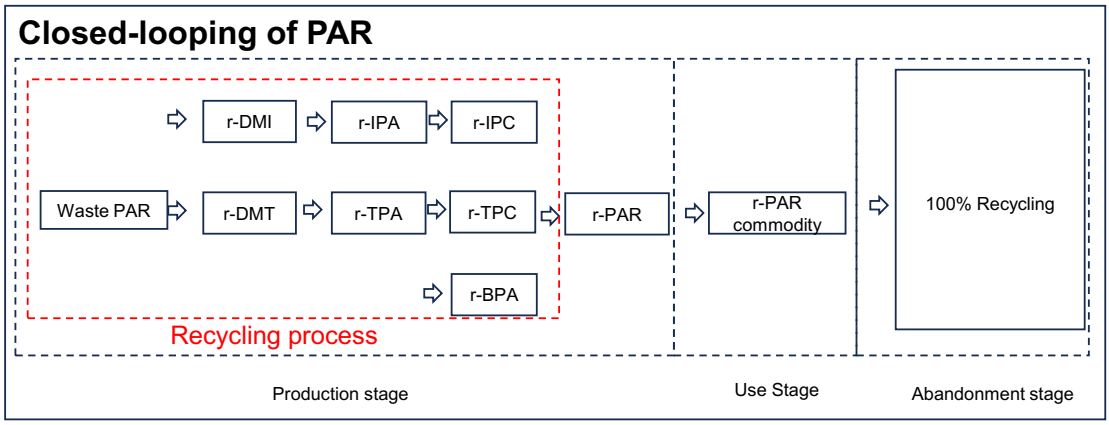

- With raw materials deduction and with recycling deduction
- The regeneration rate (*rp*) of the recycling is assumed to be 97% based on the results of the kilogram-scale experiments. .

Item	Quantity	Unit
Input: waste PET→r-DMT, r-DMI, r-BPA		
waste PAR	1	t
Electricity, low voltage	200	kWh
Heat (from steam)	4.5	t
MeOH	303	kg
Catalyst	1	kg
N_2	20	m^3
Ethyl acetate	0.5	t
Desalted water	1	t
Tap-water	1.58	t
Output:		
r-BPA	0.61	t
Mixed ester (r-DMT, r-DMI)	0.52	t

Item	Quantity	Unit
Input: r-DMT, r-DMI → r-TPC, r-IPC		
Mixed ester (r-DMT, r-DMI)	0.52	t
Electricity, low voltage	328.9	kWh
Heat (from steam)	0.729	t
Caustic soda (98%)	243.8	kg
Hydrochloric acid (31%)	536.3	kg
Sulfuric acid	10.48	kg
Dichlorosulfoxide	0.636	t
Catalyst	0.05	kg
Activated carbon	53.6	kg
Desalted water	1.6	t
Tap-water	1.305	t
Output:		
r-TPC, r-IPC	0.529	t
NaCl	0.362	t
Na_2SO_3 (30%)	49.6	kg

Item	Quantity	Unit
Input: r-PAR production		
Electricity, low voltage	212	kwh
Heat (from steam)	6.2	t
Caustic soda (98%)	0.228	t
Dichloromethane	0.131	t
N_2	20	m^3
Ethanol	4	t
Catalyst	0.1	kg
r-TPC (from waste PAR)	0.283	t
r-IPC (from waste PAR)	0.283	t
r-BPA (from waste PAR)	0.457	t
Desalted water	6	t
Tap-water	3.63	t
Output:		
r-PAR-2	1	t

Supplementary Table 9 Life-cycle environmental impact results

Impact category	Path1	Path2	Path3	Case1	Case2	Unit
Climate change (GWP)	5.93	3.26	8.55	6.32	7.24	10^3 kg CO_2 eq/ t Plastic
Primary energy demand (PED)	13.9	7.04	28.1	23.1	25.7	10^4 MJ/ t Plastic
Resource Depletion-water (WU)	5.02	2.02	6.49	3.42	12.1	10^4 kg/ t Plastic
Ecotoxicity-freshwater (ET)	35.4	6.8	59.4	18.7	22.5	10^2 CTUe/ t Plastic
Human toxicity, cancer effects (HT-cancer)	10.15	4.32	4.64	4.81	6.22	10^{-5} CTUe/ t Plastic
Resource use-fossils (ADP-fossils)	13.7	6.98	28	23.0	25.6	10^4 MJ/ t Plastic
Eutrophication-freshwater (EP-freshwater)	60.9	3.51	126	91.1	114.8	10^{-2} kg P eq/ t Plastic
EF-particulate matter (PM)	5.38	1.82	3.72	6.25	8.75	10^{-4} kg PM 2.5 eq/ t Plastic
Acidification (AP)	21.9	6.33	45.3	36.5	40.0	mol H^+ eq/ t Plastic

Supplementary Note: The economic evaluation

We configured r-PAR to achieve an annual throughput of 10,000 tons and conducted a thorough economic assessment by analyzing the mass accounting and prices of key chemicals, including TPC, EG, DMC, etc. The value-added estimation equation for the co-upcycling of PC and PET to PAR is as follows:

$$\text{Value added} = \sum \left(\text{Prices}_{\text{Input}} \times \text{Quantity}_{\text{Input}} \right) - \sum \left(\text{Prices}_{\text{output}} \times \text{Quantity}_{\text{output}} \right) \quad (8)$$

Based on the kilogram experiment, the yield of the main material was about 95%. However, EG and DMC have errors due to the nature of the material and the recovery process. Mass balance in the methanolysis, acyl chlorination, and polymerization steps are estimated to be in the range of 100 ± 15%.

Supplementary Table 10 Assumptions and parameters for the economic evaluation[7,8].

Input	**Prices [$/ton]**	**Quantities [tonne/year]**
Waste PET	571	2670
Waste PC	571	5100
MeOH	400	2690
NaOH	357	2040
HCl	171	2240
$SOCl_2$	200	1410
IPC	4000	2830
Output	**Prices [$/ton]**	**Quantities [tonne/year]**
r-PAR	10000	10000
EG	600	870
DMC	657	1120

Note: The unit price of each chemical was based on the market price at the time of calculation. Material quantities were evaluated based on actual yields during the experiment.

References

1. Hu, L. C., Oku, A. & Yamada, E. Alkali-catalyzed methanolysis of polycarbonate. A study on recycling of bisphenol A and dimethyl carbonate. *Polymer* **39**, 3841–3845 (1998).

2. Guo, J. et al. Efficient alcoholysis of polycarbonate catalyzed by recyclable Lewis acidic ionic liquids. *Ind. Eng. Chem. Res.* **57**, 10915–10921 (2018).

3. Liu, F. S. et al. Synergistic catalysis over hollow CeO_2-CaO-ZrO_2 nanostructure for polycarbonate methanolysis with methanol. *Chem. Eng. J.* **369**, 205–214 (2019).

4. Song, X. Y. et al. Methanolysis of polycarbonate into valuable product bisphenol A using choline chloride-based deep eutectic solvents as highly active catalysts. *Chem. Eng. J.* **388**, 124324 (2020).

5. PAS 2050: 2011-Specification for the Assessment of the Life Cycle Greenhouse Gas Emissions of Goods and Services. Department for Environment, Food and Rural Affairs, & British Standards Institution: United Kingdom, 2-12 (2011).

6. Nordahl, S. L. & Scown, C. D. Recommendations for life-cycle assessment of recyclable plastics in a circular economy. *Chem. Sci.* 10.1039/d4sc01340a (2024).

7. Dastidar, R. G. et al., Catalytic production of tetrahydropyran (THP): A biomass-derived, economically competitive solvent with demonstrated use in plastic dissolution. *Green Chem.* **24**, 9101–9113 (2022).

8. Redl, S., Sukumara, T., Ploeger, L., Wu, T. & Ølshøj Jensen, A. T. Nielsen, H. Noorman, Thermodynamics and economic feasibility of acetone production from syngas using the thermophilic production host Moorella thermoacetica. *Biotechnol. Biofuels* **10**, 150 (2017).